

Automatic vector signal generator calibration method suitable for multiport large-signal measurements

T. Reveyard*, A. Courty*, M. Portelance*, P. Medrel*, P. Bouysse*, J.-M. Nébus*

*XLIM, 123 av. Albert Thomas, 87060 Limoges Cedex, France

Abstract—The increasing need for measurement setups including several vector signal generators is associated with the creation of multiple input amplifiers such as digital Doherty, outphasing techniques or amplifier with a RF load matching control such as Load Modulated Balanced Amplifiers (LMBA). Therefore, an absolute calibration, in amplitude and phase of the sources has to be performed. A complete and automated calibration method for multiport generation is presented here. It introduces, as a new standard, a multiport passive device previously characterized in S-parameters. This method is detailed analytically and validated experimentally. Calibrated measurements of dual input power amplifiers are also presented.

Index Terms—instrumentation, calibration, multiport, vectorial signal generator, modulation, digital Doherty amplifier, load modulated balanced amplifier, LMBA.

I. INTRODUCTION

Recently, we have seen the emergence of multiple inputs RF power amplifiers to improve the performance of transmitters. In such power amplifiers, efficiency, linearity and bandwidth performances may outclass traditional single-input architectures. A first idea is to remove the input power divider for Doherty and/or Outphasing amplifiers [1] to digitally optimize the phase shift balance at the input of the two power transistors. This approach leads us to a dual-input amplifier named, for example, “Digital Doherty” [2], [3]. More complex multiple input structures can be developed such as: Doherty / Outphasing combinations [4], Load Modulated Balanced Amplifiers (LMBAs) [5], linearization functions using multiport digital predistortion, or the study of “Massive MIMO” systems [6]. All of those studies require the use of multiport RF modulated sources by combining several vector signal generators (VSG) sharing a common local oscillator (LO). Some measurements are presented in the literature [7], [8], but information related to the calibration procedure of the multiport source (the association of several VSGs) and particularly the phase shift control at the reference planes of the device under test is not clearly explained. This article presents a CW automatic calibration procedure of a multiport generator (association of several VSGs). Even for CW signals, VSGs sharing the same LO is necessary to ensure phase consistency and repeatability. CW signals are thus created with constant complex envelope modulations. First, a standard 1-port calibration procedure of a RF source will be described. This calibration may be on CW or multitone mode. This calibration technique, limited to a single VSG is already in use for RF envelope measurement setups. Then, we will present the extension of this calibration to an unlimited number of ports. This new automatic calibration procedure, in CW mode

only, will consider any passive multiport pre-characterized S-parameters as a standard of calibration. The new calibration method will be validated on a passive device. Finally, calibrated measurements of two dual-input RF power amplifiers will illustrate this article: a digital Doherty and a LMBA.

II. ONE-PORT SOURCE CALIBRATION

Figure 1 shows a modulated source associated with a power driver amplifier in order to characterize a non-linear power device under test (DUT). The Vector Signal Generator (VSG) includes a baseband arbitrary waveform generator to create the RF complex envelope of a desired modulation. This complex envelope can be ideally phase shifted in baseband of a value $\Delta\Phi$ given by the user. Analog signals $I(t)$ and $Q(t)$ corresponding to this phase shifted envelope will drive an IQ modulator to transpose baseband modulation in RF around a carrier frequency of interest given by the local oscillator (LO). In the case of continuous wave measurements (CW), the baseband signal is constant in magnitude and phase versus baseband time. Commercial VSG may be previously calibrated at their RF output connector reference plane. Some VSG include a software option in order to embed the reference plane of the instrument to the DUT reference plane with a Touchstone S-parameter (S2P) file of the bench (including here, 3 isolators, the driver PA and the coupler). Measurements of those S2P files may be difficult (driver PA in instrumentation may be heavy and difficult to handle), and such a method will require several connections/disconnections. Thus, a good option is to

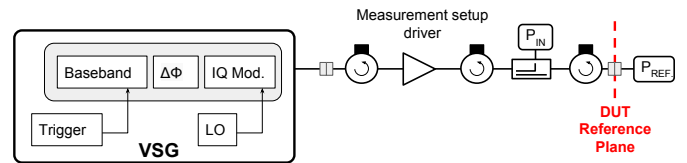


Fig. 1: One-port generator calibration in CW. The instrumentation driver has to be linear in the power range expected during measurements. Circulators ensure isolation and a 50 Ω source impedance at the DUT reference plane.

calibrate the global RF source (including the VSG, coupler, and a measurement power sensor) in power by identifying the power offset between the power sensor connected to the coupler and another one located at the DUT reference plane, measuring the 50 Ω available power. By extending this method, we can perform a source calibration by extracting the RF gain between the available power at the reference plane

and the available power that would be ideally generated by the VSG according the command entered by the user. This available gain is written as follow:

$$|G_1| = \left| \frac{a_1}{a_{s1}} \right| \quad (1)$$

where a_{s1} is the power-wave that is supposed to be generated by the source instrument and a_1 , the power-wave at the DUT reference plane. Power-wave magnitude is calculated from a given available power in dBm as:

$$|a| = \sqrt{2} \cdot 10^{\frac{P_{dBm} - 30}{20}} \quad (2)$$

The knowledge of the phase of this gain is not necessary for CW measurement as far as we measure a single input Time Invariant System such as a standard power amplifier. Nevertheless, multitone measurements (like modulated signals) of such device will require a phase calibration at each frequency. The phase of the gain, displayed in equation (1), can be obtained by using a calibrated Vector Signal Analyser (VSA) at the DUT's reference plane and calculating a ratio between ideal and measured complex envelopes in the frequency domain with a multitone signal.

III. MULTIPOINT SOURCE CALIBRATION

With a measurement setup including several RF sources, we have to complete an absolute calibration (identifying magnitude and phase of the complex gain G_i , as written in equation (1) when $i = 1$, of each RF source compared to a reference RF source. Figure 2 illustrates a general configuration of the use of several VSG simultaneously at a common frequency (LO). Let's assume the VSG number 1 is already calibrated as explained in part II. Therefore, the power-wave a_1 , at the input port 1 reference plane is known. The idea for the multiple-input calibration consists in using a passive multiport, preliminary characterized, for which the S-parameters are totally known and available with a SnP file. The VSG number 1, our reference path, remains on, during our multiport calibration. Other RF paths will be calibrated independently and sequentially.

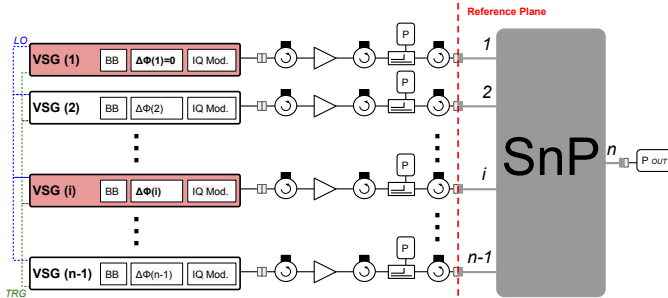


Fig. 2: Multiport generator calibration in CW.

When active channels are connected to ports 1 and i of the SnP, the output power-wave can be written as:

$$b_n = S_{n1} \cdot a_1 + S_{ni} \cdot a_i \quad (3)$$

where a_1 are a_i are the power-waves at the active inputs of the combiner, respectively on port 1 and i . A power measurement at the output of the combiner will give us, according to equation (2), $|b_n|^2$ that can be expressed as:

$$|b_n|^2 = |S_{n1} \cdot a_1 + S_{ni} \cdot G_i \cdot a_{si}|^2 \quad (4)$$

Expending (4) can be written as:

$$\begin{aligned} A \cdot |G_i|^2 + B \cdot \Re\{G_i\} + C \cdot \Im\{G_i\} &= D \\ \text{with} \\ A &= |S_{ni} \cdot a_{si}|^2 \\ B &= 2 \cdot \Re\{S_{n1}^* \cdot a_1^* \cdot S_{ni} \cdot a_{si}\} \\ C &= -2 \cdot \Im\{S_{n1}^* \cdot a_1^* \cdot S_{ni} \cdot a_{si}\} \\ D &= |b_n|^2 - |S_{n1} \cdot a_1|^2 \end{aligned} \quad (5)$$

A , B , C , and D are full-known terms. $a_{si} = |a_{si}| \cdot e^{j \cdot \Delta \Phi_i}$ is the power-wave from the source number i : its phase is $\Delta \Phi_i$ and its magnitude is calculated from equation (2) from the user command related to its power level. Equation (5) is a 3-unknowns linear equation. Those unknowns may be found out by solving the linear system build on 3 independants $\Delta \Phi_i$ values: ϕ_A, ϕ_B, ϕ_C . Considering more values will give a least-square solution.

$$\begin{pmatrix} |G_i|^2 \\ \Re\{G_i\} \\ \Im\{G_i\} \end{pmatrix} = \begin{bmatrix} A(\phi_A) & B(\phi_A) & C(\phi_A) \\ A(\phi_B) & B(\phi_B) & C(\phi_B) \\ A(\phi_C) & B(\phi_C) & C(\phi_C) \\ \vdots & \vdots & \vdots \end{bmatrix}^\dagger \cdot \begin{pmatrix} D(\phi_A) \\ D(\phi_B) \\ D(\phi_C) \\ \vdots \end{pmatrix} \quad (6)$$

where \bullet^\dagger denotes the pseudo-inverse operator.

G_i complex value is then automatically extracted for each RF frequency. This procedure is performed for each RF source added to our reference one connected to port 1 of our SnP standard.

IV. EXPERIMENTAL CW VALIDATION OF THE CALIBRATION METHOD

Figure 3 shows an experimental validation of the calibration procedure on a commercial 2-channel VSG and a power combiner pre-characterized in S-parameters. Measurement results are displayed in figure 4. Each curve stands for one RF frequency (7 frequencies from 2.2 GHz up to 2.8 GHz with a 100 MHz step). The blue curves show, at each frequency, the power measured at the output of the combiner versus $\Delta \Phi$ applied to the VSG (without any phase calibration). The black curves illustrate the same measurements when the phase calibration is taken into account: $\Delta \Phi$ is the phase of the wave a_2 at the DUT reference plane assuming that the phase of a_1 is zero (port 1 is our phase reference). Finally, red curves depict output power versus $\Delta \Phi$ simulation traces, calculated from the combiner S3P file, $\Delta \Phi$ value and input power-waves magnitudes $|a_1|$ and $|a_2|$ measured at the input of the combiner. A good agreement between our calibrated measurements and the associated simulation can be observed.

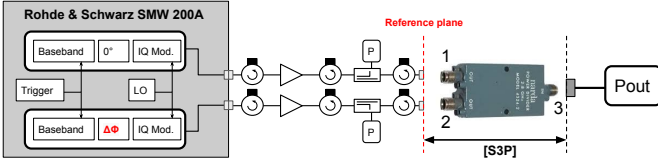


Fig. 3: Bench for the calibration verification.

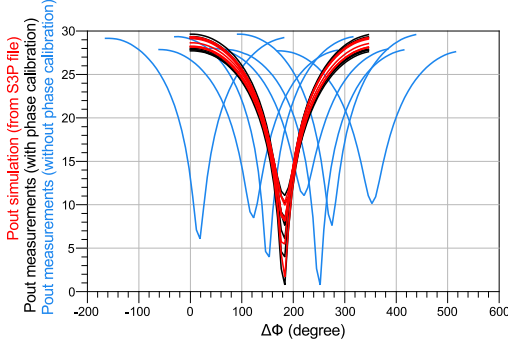


Fig. 4: Power at the output of the combiner depicted on fig. 3 for seven RF frequencies. The dual source measurement results are performed without a phase calibration (blue), with a phase calibration (black) and compared to simulations (red).

V. APPLICATION TO DUAL-INPUT POWER AMPLIFIER CW MEASUREMENTS

The proposed calibration method is applied in the framework of dual-input power amplifier characterizations. Two calibrated measurement examples complete this paper: a digital Doherty and a LMBA presented on figures 5 and 8 respectively. Measurement results will highlight the effects of the power (ΔP) and phase ($\Delta\varphi$) offsets between the two inputs. Those offsets can be expressed from power-waves as:

$$\Delta\varphi (^{\circ}) = \text{Arg} \left\{ \frac{a_{in 2}}{a_{in 1}} \right\} \quad (7)$$

$$\Delta P (\text{dB}) = 10 \log_{10} \left(\frac{|a_{in 2}|^2}{|a_{in 1}|^2} \right)$$

During large-signal characterization, for each available power

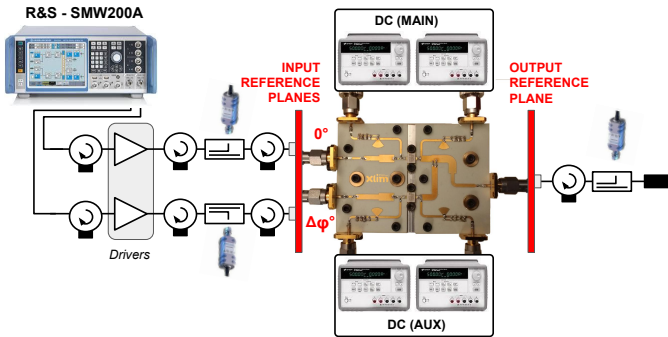


Fig. 5: Measurement setup for the CW measurements of a digital Doherty power amplifier (dual-input).

presented at the main input of the DUT, sweeps are performed on ΔP and $\Delta\varphi$. Regarding measurement results presented here, drain efficiency (DE) and power added efficiency (PAE) are calculated from power in Watt as follow:

$$DE(\%) = 100 \cdot \frac{P_{out}}{P_{DC}}$$

$$PAE(\%) = 100 \cdot \frac{P_{out} - (P_{in 1} + P_{in 2})}{P_{DC}} \quad (8)$$

A. Digital Doherty Amplifier

The measured digital Doherty amplifier has been fabricated on a Rogers 4350B substrate using two CGH410F GaN transistors from Wolfspeed. The main stage is biased in class AB and the auxiliary in class C.

The purpose of the large signal measurements is to find out the best digital control (ΔP and $\Delta\varphi$ as function of power) for the fabricated Doherty. Figure 6 presents the performances of the PA at 2.3 GHz. From those measurements, we can extract the best behavior for efficiency (curve 1 colored in red) or linearity (curve 2 colored in green). Each optimal behavior is associated with a unique digital control that can be plotted as a function of the output power (figure 7)

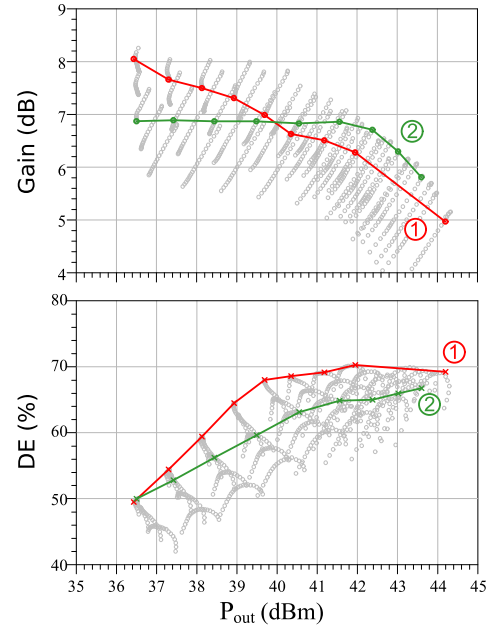


Fig. 6: Digital Doherty gain and drain efficiency CW measurements at 2.3 GHz.

B. Load Modulated Balanced Amplifier (LMBA)

In order to illustrate the capabilities of our calibrated measurement setup, we have created a raw Load Modulated Balanced Power Amplifier (LMBA) from commercially available circuits: two demonstration amplifier circuits CGH27015-TB from Cree/Wolfspeed and two connectorized 90° hybrid couplers IPP 2122 from Innovative Power Products. GaN transistors are biased in class-AB ($V_{ds0} = 28 \text{ V}$ and $I_{ds0} = 70 \text{ mA}$). The nominal gain of each PA is 14.7 dB at 2.4 GHz and

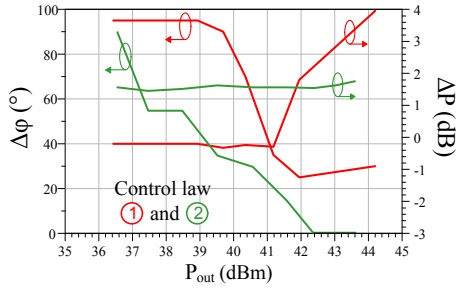


Fig. 7: Digital control optimizing the digital Doherty amplifier for efficiency (1) or linearity (2).

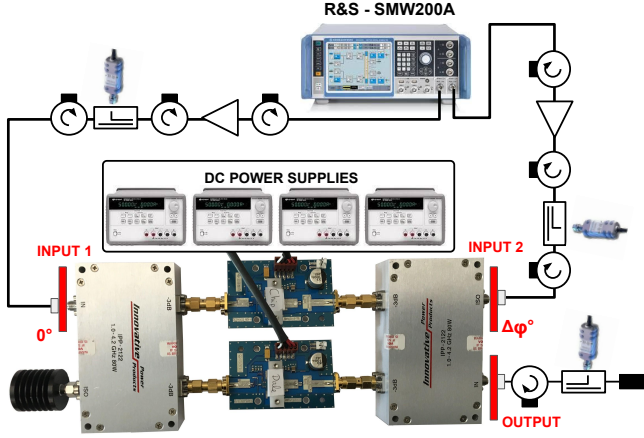


Fig. 8: Measurement setup for the CW measurements of a Digital (dual-input) Load Modulated Balanced Amplifier (LMBA).

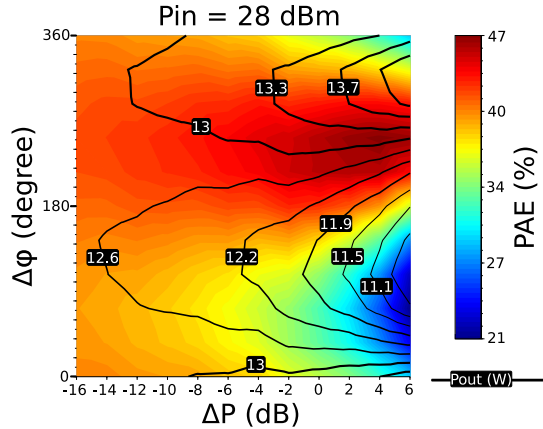


Fig. 9: Global performances of the LMBA, including two PAs and couplers, depicted on figure 8 at $f_0 = 2.4$ GHz for an input available power $P_{in} = 28$ dBm. Contours are based on measurement samples uniformly distributed on this surface with a 2 dB step for ΔP and 15° for $\Delta\varphi$. Lines are output power isocurves in Watts. The jet colorbar indicates the power added efficiency.

the 1dB-compression point is reached for an input available power of 20 dBm.

The measurement setup and the LMBA under test are illustrated on figure 8. The idea is to identify the best CW signal (amplitude and phase) to be injected at the INPUT 2 reference plane in order to optimize the behavior of the two main amplifiers. A measurement result example is presented on figure 9. This plot superimposes the PAE and output power performance in the $\{\Delta P; \Delta\varphi\}$ plane.

Those dual input LMBA measurements are a prime of importance for the implementation of an optimized control path (phase shifter and control PA) when the designer has to release a single input LMBA as in [9].

VI. CONCLUSION

This paper presents an automated calibration method to apply when several VSG sharing the same local oscillator are associated simultaneously within a bench. This method takes the advantage to consider any pre-characterized multi-port passive circuit as a standard. The calibration procedure has been presented analytically, validated experimentally and finally applied for large signal measurements of two dual-input power amplifiers in S-band:

- a digital Doherty and investigations on the control law expected for the input combiner ;
- a Load Modulated Balanced Amplifier (LMBA) and a direct plot of the AM/PM of the auxiliary path to add.

Those measurements require an accurate characterization of the phase offset between the inputs of the power amplifiers in order to optimize the amplifiers behaviors in terms of efficiency or linearity. Such measurements are possible with the proposed calibration method and offer an experimental view on the ideal input combiner function expected by the designer.

REFERENCES

- [1] C. M. Andersson *et al.*, "A 1–3-GHz Digitally Controlled Dual-RF Input Power-Amplifier Design Based on a Doherty-Outphasing Continuum Analysis," *IEEE Transactions on Microwave Theory and Techniques*, vol. 61, no. 10, pp. 3743–3752, Oct 2013.
- [2] R. Darraji *et al.*, "A Dual-Input Digitally Driven Doherty Amplifier Architecture for Performance Enhancement of Doherty Transmitters," *IEEE Transactions on Microwave Theory and Techniques*, vol. 59, no. 5, pp. 1284–1293, May 2011.
- [3] A. Piacibello *et al.*, "Dual-input driving strategies for performance enhancement of a doherty power amplifier," in *IEEE MTT-S International Wireless Symposium (IWS)*, May 2018, pp. 1–4.
- [4] A. R. Qureshi *et al.*, "A 112W GaN dual input Doherty-Outphasing Power Amplifier," in *IEEE MTT-S International Microwave Symposium (IMS)*, May 2016.
- [5] D. J. Sheppard *et al.*, "An efficient broadband reconfigurable power amplifier using active load modulation," *IEEE Microwave and Wireless Components Letters*, vol. 26, no. 6, pp. 443–445, June 2016.
- [6] W. Chen *et al.*, "Energy-efficient doherty power amplifier MMIC and beamforming-oriented digital predistortion for 5G massive MIMO application," in *IEEE Asia-Pacific Microwave Conference (APMC)*, Nov 2017, pp. 391–394.
- [7] R. Quaglia and S. Cripps, "A load modulated balanced amplifier for telecom applications," *IEEE Transactions on Microwave Theory and Techniques*, vol. 66, no. 3, pp. 1328–1338, March 2018.
- [8] R. Kalyan *et al.*, "A Digitally Assisted Dual-Input Dual-Band Doherty Power Amplifier With Enhanced Efficiency and Linearity," *IEEE Transactions on Circuits and Systems II: Express Briefs*, vol. 66, no. 2, pp. 297–301, Feb. 2019.
- [9] P. H. Pednekar *et al.*, "Analysis and Design of a Doherty-Like RF-Input Load Modulated Balanced Amplifier," *IEEE Transactions on Microwave Theory and Techniques*, vol. 66, no. 12, pp. 5322–5335, Dec 2018.